Clays and Clay Minerals, Vol. 34, No. 2, 125–135, 1986.

PATHWAYS OF SMECTITE ILLITIZATION

CRAIG M. BETHKE, NORMA VERGO, AND STEPHEN P. ALTANER
Department of Geology, University of Illinois
Urbana, Illinois 61801

Abstract—Junction probability diagrams show variation in both composition and layer arrangement in mixed-layer clay minerals. These diagrams can represent short-range and long-range ordered, random, and segregated interstratifications. Mineralogical analyses of illite/smectite from shale cuttings, bentonites, and hydrothermally altered tuffs define characteristic reaction pathways through these diagrams. Shale and bentonite analyses fall along pathways joining smectite and illite on diagrams showing nearest-neighbor (R1) layer arrangements. Transition from random to R1-ordered interstratifications occurs in shale samples containing 60–70% illite layers, and in bentonites containing 55–67% illite layers. Analyses of alteration products, however, fall near a line connecting rectorite and illite, which represents the maximum degree of R1 layer ordering. No mineralogical evidence is available to suggest that these alteration samples formed from a smectite precursor. All samples develop next-nearest (R2) and thrice-removed (R3) neighbor ordering along similar pathways. Transition to R2 ordering occurs gradually in samples composed of 65–80% illite layers, and samples containing more than 85% illite layers may show strong R3 ordering.

Key Words—Illite/smectite, Illitization, Junction probability diagram, Mixed layer, Ordering, Smectite.

INTRODUCTION

Illite/smectite (I/S) is a common mixed-layer or interstratified clay mineral (Weaver, 1956, 1959) composed of illite and smectite layers arranged in stacking sequences along the crystallographic c^* axis (Reynolds, 1980). Smectite layers differ principally from illite layers by smaller negative charges on the silicate sheets, the presence of water and exchangeable cations in interlayer positions, and their expandability in water and some organic solvents. I/S varies both in composition, i.e., the proportion of illite to smectite layers, and in the arrangement of layers within stacking sequences.

Many workers have observed that I/S in shales (Perry and Hower, 1970; Weaver and Beck, 1971; Boles and Franks, 1979) and bentonites (Rettke, 1976) becomes progressively richer in illite layers and poorer in smectite layers with increased depths of burial in sedimentary basins. This process is herein referred to as smectite illitization. In addition, based on analysis of X-ray powder diffraction patterns, I/S develops increasing degrees of layer ordering during illitization (Reynolds and Hower, 1970; Perry and Hower, 1970). Randomly interlayered minerals (R0 ordering, in the abbreviated notation of Reynolds, 1980) alter to short-range (R1) and then long-range (R2 and R3) ordered phases, generally at temperatures of 100°C or greater (Weaver and Beck, 1971; Hower *et al.*, 1976). Nadeau and Reynolds (1981), Horton (1983), and Vergo (1984) also observed illitization and the development of ordering in I/S due to contact metamorphism and hydrothermal alteration.

In this paper, we introduce junction probability diagrams, which show composition and layer arrangement in mixed-layer minerals, and use these diagrams to define reaction pathways of smectite illitization in shales, bentonites, and hydrothermally altered tuffs.

JUNCTION PROBABILITY DIAGRAMS

Junction probability diagrams conveniently show variation of composition and layer arrangement in mixed-layer minerals. Junction probabilities are statistical parameters used to describe stacking sequences within mixed-layer minerals for X-ray powder diffraction (XRD) calculations (MacEwan, 1956, 1958; Reynolds, 1980). Probabilities vary from zero to one and are commonly derived by successfully modeling a mineral's XRD pattern.

Nearest-neighbor layer arrangements

Plots of $P_{I,I}$, the probability of an illite layer following a given illite layer in a sample, vs. P_I, the fraction of illite layers, show the amount of segregation or ordering present in R1 layer arrangements, often called nearest-neighbor arrangements, in I/S. Such plots fully describe R1 arrangements, because, by relations among junction probabilities (Reynolds, 1980, Eqs. (1)–(4)), specifying P_I and $P_{I,I}$ fixes values of all other variables (P_S, $P_{I,S}$, $P_{S,I}$, $P_{S,S}$).

In a plot of $P_{I,I}$ vs. P_I, pure smectite and illite occupy the lower left and upper right corners of the diagram (Figure 1). Randomly interlayered (R0) I/S minerals fall along the diagonal between these two points, because by definition, $P_{I,I} = P_I$. Because $P_{I,I} > P_I$ requires a tendency toward clustering of illite layers from smectite layers, points above the diagonal represent segregated interstratifications. Degree of segregation increases toward the line $P_{I,I} = 1$, which describes a physical mixture of illite and smectite crystallites.

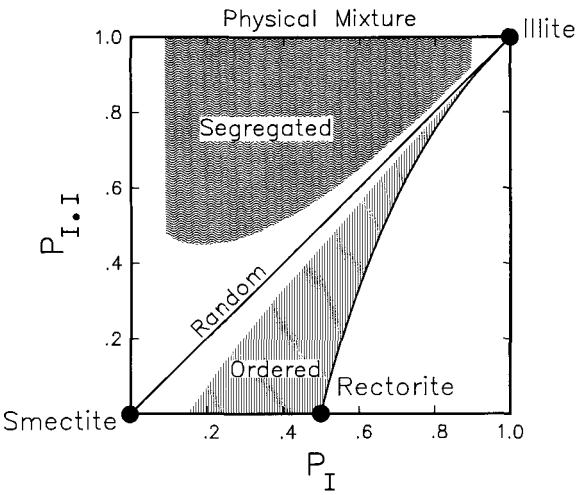

Figure 1. Junction probability diagram showing regions of R1-segregated, random, and R1-ordered layer arrangements. Illite and smectite occupy upper right and lower left corners of diagram. Random interlayerings occur on diagonal between these points. Segregated minerals plot above, and ordered minerals plot below diagonal. Maximum segregation is physical mixture, at top of diagram. Greatest ordering falls along the line between smectite and rectorite, and then along the curve defined by Eq. (1) from rectorite to illite. No rational arrangements fall to right of this curve.

Points below the diagonal represent ordered arrangements, because $P_{I.I} < P_I$ requires that illite and smectite layers tend to alternate. Point $P_I = .5$, $P_{I.I} = 0$ describes perfect alternation, represented in nature by K-rectorite, a perfectly ordered I/S mineral (Bradley, 1950; Brindley, 1956). Line $P_{I.I} = 0$, connecting smectite with rectorite, defines maximum ordering in I/S containing less than 50% illite layers. I/S minerals with more than 50% illite layers have the greatest degree of ordering along the line

$$P_{I.I} = \frac{2P_I - 1}{P_I}, \quad \text{where} \quad P_I \geqq .5, \qquad (1)$$

which is derived from the condition $P_{S.I} = 1$. Points to the right of this line describe irrational ordering in which some junction probabilities do not fall in the range zero to one. For example, it is not possible to arrange the layers in an illite-rich mineral so that there is little likelihood of illite layers neighboring illite layers.

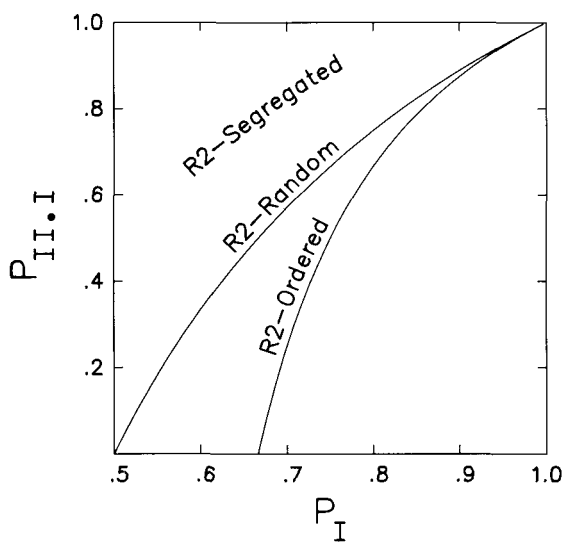

Figure 2. Junction probability diagram for R2 layer arrangements in fully R1-ordered minerals. Labeled lines show R2-random (Eq. (1)) and R2-ordered (Eq. (2)) interlayerings. Partially R2-ordered arrangements fall between these lines, and R2-segregated arrangements plot above random line.

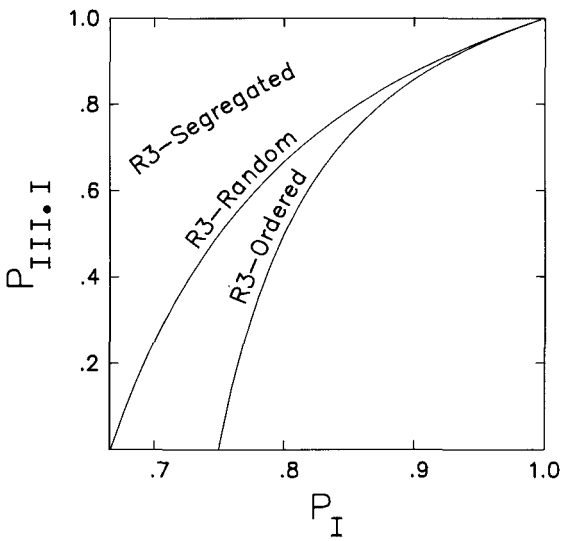

Figure 3. Junction probability diagram for R3 layer arrangements in fully R1- and R2-ordered minerals, showing lines for R3-random (Eq. (2)) and R3-ordered (Eq. (3)) interlayerings, and region of R3 segregation.

In practice, minerals may deviate somewhat from the R0 diagonal without showing XRD evidence of segregation or ordering. Patterned areas in Figure 1 show regions of the junction probability diagram in which segregation and ordering produce important diffraction effects.

Next-nearest neighbor arrangements

Eight additional junction probabilities ($P_{II.I}$, $P_{II.S}$, $P_{IS.I}$, etc.) describe R2 or next-nearest neighbor layer arrangements. Six relations may be written among these variables (Reynolds, 1980, p. 253), leaving two additional required values. If maximum R1 ordering is present before R2 ordering occurs, as seems to exist in I/S, four probabilities and three relations may be eliminated, leaving only one degree of freedom.

The R2 layer arrangement in I/S with maximum R1 order, then, may be represented in a junction proba-

https://doi.org/10.1346/CCMN.1986.0340203 Published online by Cambridge University Press

Table 1. Estimation of predominant ordering from position of low-angle peak (data of Reynolds, 1980).

Ordering	d (Å)	°2θ[1]
R1	14.5–12.8	6.1–6.9
R2	12.8–11.5	6.9–7.6
R3	11.5–10.5	7.6–8.4

[1] λ = 1.54 Å.

bility diagram of $P_{II.I}$ vs. P_I (Figure 2). In this type of diagram, line $P_{II.I} = P_{I.I}$, where $P_{I.I}$ in R1-ordered I/S is given by Eq. (1), represents R2-random interlayering. R2-random interlayering, which describes disorder among next-nearest neighbors in R1-ordered minerals, should not be confused with the random arrangement of nearest neighbors in fully disordered I/S. Maximum R2 ordering occurs when

$$P_{II.I} = \frac{3P_I - 2}{2P_I - 1}, \quad \text{where} \quad P_I \geqq .667, \qquad (2)$$

which is derived by setting $P_{SI.I} = 1$. Points between the R2-random and R2-ordered lines represent partial R2 ordering, and points above the R2-random line show R2 segregation. Line $P_{II.I} = 1$ describes maximum R2 segregation, which is a mixture of K-rectorite and illite crystallites.

Thrice-removed neighbor arrangements

Sixteen additional junction probabilities ($P_{III.I}$, $P_{III.S}$, $P_{IIS.I}$, etc.) and thirteen additional relations describe R3 or thrice-removed neighbor arrangments (Reynolds, 1980, p. 254). Three additional values are required unless maximum R1 and R2 ordering is assumed. Here, twelve probabilities and ten equations may be eliminated, and R3 arrangements are fully described on a plot of $P_{III.I}$ vs. P_I (Figure 3).

Line $P_{III.I} = P_{II.I}$, where $P_{II.I}$ is given by Eq. (2), gives R3-random interlayering, in which there is no tendency for ordering among thrice-removed neighbors. Maximum R3 ordering occurs along

$$P_{III.I} = \frac{4P_I - 3}{3P_I - 2}, \quad \text{where} \quad P_I \geqq .75, \qquad (3)$$

from setting $P_{SII.I} = 1$. Partial R3 ordering falls between these lines, and R3 segregation lies above the R3-random line.

MINERALOGICAL ANALYSIS

To define precisely pathways of smectite illitization in nature, 142 published and unpublished XRD patterns of I/S were analyzed using methods of Reynolds (1980) and Środoń (1984). Where possible, samples were chosen from suites with broad ranges of illite content. Predominant ordering, the shortest range of ordering which describes diffraction from a mineral, was estimated from position of the low-angle peak between 10.5 and 14.5 Å in ordered samples (Table 1), and then confirmed by diffraction modeling. Values of P_I, $P_{I.I}$, $P_{II.I}$, and $P_{III.I}$ are reported here which give the most successful modeled diffraction patterns from 2° to 30°2θ, using the MOD-4 computer program written by R. C. Reynolds (Dartmouth College, Hanover, New Hampshire). This modeling assumed a single I/S phase, and the calculations considered crystallite thicknesses of no more than 13 layers, due to computational constraints. Calculations also used a random powder Lorentz factor, crystallite sizes of 7–13 layers in equal proportions, 0.8 K atoms per illite half-unit cell, 0.2 Fe atoms per I/S half-unit cell, and smectite and illite layer thicknesses of 16.9 and 10.0 Å, respectively. Uncertainty in determinations of P_I was about ±0.02–0.03. To represent approximate uncertainties in the analyses, the ranges of junction probabilities which give reasonable diffraction models are also reported. Tables 2–4 list results from analysis of I/S from 29 shales, 51 bentonites, and 62 hydrothermally altered tuffs.

DISCUSSION

Mineralogical analyses of I/S samples follow distinct pathways through junction probability diagrams. Figure 4 shows shale, bentonite, hydrothermal, and combined results plotted on R1 diagrams. Analyses of I/S from shales and bentonites define a pathway from smectite to illite which crosses from random to ordered interlayering. Samples containing <55% illite layers are randomly interstratified and straddle the R0 diagonal. These samples may contain small amounts of segregation without significantly altering their XRD patterns. Shale and bentonite samples containing 55–70% illite layers fall on or between the random and R1-ordered lines, and generally show increased layer ordering with greater illite content. I/S with >70% illite layers is mostly or completely R1-ordered.

Transition from random to ordered interlayerings occurs in shale samples which contain 60–70% illite layers and in bentonites which contain 55–67% illite. This slight difference may be due to small amounts of detrital illite in shale samples studied, which could have inflated estimates of P_I, or to dissimilar origins of I/S in shales and bentonites.

Many shale and bentonite analyses in this range of illite content fall between the random and ordered lines, suggesting that transition from random to ordered interlayerings may be a continuous process, rather than a distinct phase change. Alternatively, these samples may contain mixtures of random and ordered I/S.

Unlike I/S from shales and bentonites, the hydrothermal I/S analyses fall along a pathway between rectorite and illite, following the line of maximum R1 ordering. There is no evidence that I/S in hydrothermal environments forms by illitization of a smectitic precursor, as is observed in diagenetic environments. In-

Table 2. Predominant ordering, fraction of illite layers, and best-fit junction probabilities for 29 shale samples.[1]

Sample[2]	Ordering	P_I	$P_{I,I}$	$P_{II,I}$	$P_{III,I}$
B-5210	R0	.17	.17 (.06–.40)		
B-6210	R0	.25	.25 (.17–.42)		
E-6201	R0	.27	.27 (.19–.43)		
C-6517	R0	.27	.27 (.19–.43)		
D-2010	R0	.30	.30 (.23–.44)		
B-7203	R0	.30	.30 (.23–.44)		
A-3000	R0	.30	.30 (.23–.44)		
E-7418	R0	.40	.40 (.36–.485)		
C-9504	R0	.40	.40 (.36–.48)		
A-7000	R0	.40	.40 (.36–.48)		
D-10020	R0	.45	.45 (.41–.51)		
E-7856	R0	.47	.47 (.43–.53)		
B-8200	R0	.47	.47 (.43–.53)		
A-11000	R0	.47	.47 (.43–.53)		
E-8379	R0	.48	.48 (.44–.535)		
D-11995	R0	.50	.50 (.46–.54)		
D-13985	R0	.52	.52 (.49–.56)		
E-8750	R0	.55	.550 (.525–.590)		
B-10222	R0	.55	.550 (.525–.590)		
A-12000	R0	.57	.570 (.550–.605)		
C-13504	R0	.58	.580 (.560–.610)		
E-9495	R0	.60	.600 (.580–.620)		
B-11240	R0	.60	.580 (.560–.600)		
E-10080	R0	.63	.600 (.580–.620)		
C-15509	R0	.63	.600 (.580–.620)		
E-10725	R1	.70	.572 (.572–.590)	.572 (.540–.572)	
C-17358	R1	.70	.630 (.620–.650)		
B-12500	R1	.70	.590 (.572–.614)		
GM-13-36[3]	R3	.90	.889	.875	.870 (.866–.874)

[1] Fine size fraction (mostly <1 μm), oriented mount, glycolated; parentheses = range of adequate fits.
[2] From Perry (1969) and Perry and Hower (1970), Texas Gulf Coast, unless otherwise noted.
[3] E. A. Perry and J. Hower, personal communication, Texas Gulf Coast.

https://doi.org/10.1346/CCMN.1986.0340203 Published online by Cambridge University Press

Table 3. Predominant ordering, fraction of illite layers, and best-fit junction probabilities for 51 bentonite samples.[1]

Sample[2]	Ordering	P_I	$P_{I,I}$	$P_{II,I}$	$P_{III,I}$
1631/4965.5[3]	R0	.15	.15 (.05–.40)		
2208/5328[3]	R0	.15	.15 (.05–.40)		
1418/5064.5[3]	R0	.38	.38 (.34–.47)		
1631/4895[3]	R0	.38	.38 (.34–.47)		
1416/6806[3]	R0	.38	.38 (.34–.47)		
1416/6803[3]	R0	.43	.43 (.385–.50)		
1628/4228[3]	R0	.43	.40 (.36–.46)		
4867/6803.7[3]	R0	.48	.48 (.44–.535)		
1634/6958[3]	R0	.53	.51 (.48–.54)		
DRP[4]	R1	.55	.183 (.183–.240)	.183 (.160–.183)	
SA-82-1610A	R1	.57	.340 (.320–.380)		
SA-82-16-6A	R1	.59	.370 (.345–.400)		
SA-82-16-7	R1	.59	.370 (.345–.400)		
SA-82-1611B	R1	.60	.430 (.410–.455)		
SA-82-1611C	R1	.60	.375 (.350–.405)		
SA-82-1610B	R1	.60	.375 (.350–.405)		
SA-82-13A	R1	.61	.385 (.370–.410)		
SA-82-11C	R1	.62	.415 (.390–.440)		
SA-82-14A	R1	.62	.415 (.390–.440)		
SA-82-12B	R1	.64	.500 (.480–.520)		
SA-82-11A	R1	.65	.525 (.500–.560)		
SA-82-12A	R1	.65	.525 (.500–.560)		
SA-82-12D	R1	.65	.525 (.500–.560)		
270D-35DAYS[5]	R1	.65	.550 (.530–.580)		
SA-82-12C	R1	.66	.535 (.510–.570)		
SA-82-11B	R1	.66	.535 (.510–.570)		
SA-82-12E	R1	.67	.530 (.495–.560)		
22-23-1[6]	R2	.70	.572	.483 (.460–.536)	
SA-82-18A	R1	.70	.572 (.572–.590)	.572 (.540–.572)	

https://doi.org/10.1346/CCMN.1986.0340203 Published online by Cambridge University Press

Table 3. Continued.

Sample[2]	Ordering	P_I	$P_{I,I}$	$P_{II,I}$	$P_{III,I}$
SA-82-18D	R1	.72	.612 (.612–.650)	.612 (.587–.612)	
3-1[6]	R2	.73	.631	.576 (.555–.598)	
LT-24[7]	R2	.73	.631	.576 (.555–.598)	
26-171[6]	R2	.74	.649	.602 (.583–.621)	
SA-7	R2	.74	.649	.583 (.564–.602)	
KB-7[8]	R2	.76	.685	.626 (.612–.641)	
SA-9	R2	.76	.685	.633 (.619–.648)	
26-65[6]	R2	.83	.795	.769 (.764–.774)	
26-59[6]	R2	.83	.795	.769 (.764–.774)	
Kalkberg[9]	R3	.86	.837	.806	.783 (.771–.794)
SA-82-36B	R3	.86	.837	.806	.783 (.771–.794)
SA-82-38	R2	.86	.837	.806 (.806–.814)	.806 (.794–.806)
SA-82-36A	R3	.87	.851	.825	.806 (.797–.815)
SA-82-36C	R3	.87	.851	.825	.806 (.797–.815)
LTE-23[7]	R3	.88	.864	.842	.820 (.813–.828)
SA-82-37C	R3	.88	.864	.842	.813 (.813–.820)
SA-82-39A	R3	.89	.877	.859	.848 (.842–.854)
SA-82-37B	R3	.90	.889	.875	.862 (.858–.866)
SA-82-29	R3	.93	.925	.919	.915 (.913–.917)
SA-82-23	R3	.97	.969	.968	.967 (.967–.970)
SA-82-24	R3	.97	.969	.968	.967 (.967–.970)
SA-82-32R	R3	.97	.969	.968	.967 (.967–.970)

[1] Fine size fraction (mostly <1 μm), oriented mount, glycolated. Parentheses = range of adequate fits.
[2] From Montana Disturbed Belt, described by Altaner *et al.* (1984) and Altaner (1985), unless otherwise noted.
[3] From Rettke (1976), Denver basin.
[4] From Pevear *et al.* (1980), British Columbia, shows rectorite-type ordering.
[5] Roberson and Lahann (1981), experimentally illitized bentonite.
[6] Brun and Chagnon (1979), southern Quebec.
[7] Hoffman (1976), Montana Disturbed Belt.
[8] Huff and Türkmenöglü (1981), Cincinnati arch.
[9] Hower and Mowatt (1966), Kalkberg, New York, shows Kalkberg-type ordering of Reynolds and Hower (1970).

stead, I/S in hydrothermally altered rocks may form by illitization of a rectorite-like phase.

Sample DRP, a K-rectorite, is an unusual bentonite because it contains only 55% illite layers and is fully R1 ordered. This sample, which formed by alteration of smectite during contact metamorphism (Pevear *et al.*, 1980), together with the hydrothermal alteration samples, may define a reaction pathway favored by I/S

https://doi.org/10.1346/CCMN.1986.0340203 Published online by Cambridge University Press

Table 4. Predominant ordering, fraction of illite layers, and best-fit junction probabilities for 62 samples of hydrothermal alteration.[1]

Sample[2]	Ordering	P_I	$P_{I,I}$	$P_{II,I}$	$P_{III,I}$
13-18.3	R1	.60	.334 (.334–.360)	.334 (.202–.334)	
13-5.2P	R1	.63	.413	.502 (.443–.560)	
13-5.5P	R1	.63	.413	.560 (.502–.619)	
13-8.8	R1	.63	.413	.502 (.443–.560)	
13-46.0	R1	.63	.413	.502 (.443–.560)	
13-53.0	R1	.63	.413 (.413–.434)	.413 (.330–.413)	
10-56.1	R1	.65	.462 (.462–.489)	.462 (.431–.462)	
10-31.1	R1	.65	.462	.516 (.462–.570)	
13-57.3	R1	.65	.462	.516 (.462–.570)	
10-52.7	R1	.66	.485 (.485–.502)	.485 (.431–.485)	
10-11.4	R2	.67	.508	.389 (.341–.436)	
13-61.3	R1	.67	.508 (.508–.524)	.508 (.460–.508)	
12-0	R2	.70	.572	.440 (.411–.483)	
12-29.6	R2	.70	.572	.536 (.483–.572)	
10-46.0	R2	.70	.572	.540 (.483–.572)	
10-21.3	R2	.70	.572	.540 (.508–.572)	
10-27.4	R1	.71	.592 (.592–.603)	.592 (.564–.592)	
NV-W-32-83	R2	.71	.592	.625 (.578–.665)	
10-67.7	R1	.72	.612 (.612–.650)	.612 (.587–.612)	
10-59.1	R1	.72	.612 (.612–.650)	.612 (.587–.612)	
10-19.2	R1	.72	.612 (.612–.650)	.612 (.587–.612)	
10-4.0	R2	.72	.612	.587 (.560–.612)	
12-23.8	R1	.73	.645 (.640–6.50)		
12-47.9	R2	.73	.631	.598 (.576–.619)	
12-36.9	R1	.74	.649 (.649–.653)	.649 (.640–.649)	
10-48.7	R2	.74	.649	.630 (.602–.649)	
10-15.8	R2	.74	.649	.630 (.611–.649)	
10-0.3	R2	.74	.649	.554 (.535–.573)	
12-5.5	R2	.75	.667	.620 (.606–.639)	

https://doi.org/10.1346/CCMN.1986.0340203 Published online by Cambridge University Press

Table 4. Continued.

Sample[2]	Ordering	P_I	$P_{I,I}$	$P_{II,I}$	$P_{III,I}$
10-62.2	R2	.75	.667	.620 (.609–.642)	
12-17.2	R1	.76	.703 (.696–.711)		
12-53.3	R2	.76	.685	.612 (.597–.626)	
10-7.6	R1	.76	.685 (.685–.692)	.685 (.670–.685)	
12-33.5	R2	.78	.718	.663 (.652–.674)	
12-58.8	R2	.78	.718	.638 (.624–.663)	
12-68.0	R2	.78	.718	.691 (.680–.702)	
10-41.5	R2	.78	.718	.707 (.691–.718)	
NV-H-12-83	R2	.78	.718	.608 (.608–.630)	.608 (.558–.608)
12-40.8P	R2	.80	.750	.667 (.667–.675)	.667 (.651–.667)
12-64.6	R2	.80	.750	.709 (.700–.730)	
13-.2	R1	.80	.750 (.750–.755)	.750 (.742–.750)	
13-71.0	R2	.80	.750	.667 (.667–.675)	.667 (.651–.667)
NV-Y-34-83	R2	.81	.766	.694 (.694–.708)	.694 (.667–.694)
12-36.9	R3	.83	.795	.743	.721 (.712–.730)
12-11.0	R3	.84	.810	.765	.762 (.755–.765)
NV-Z-35-83	R3	.86	.837	.806	.783 (.771–794)
NV-AA-36-83	R3	.87	.851	.825	.797 (.788–.806)
NV-AC-38-83	R3	.87	.851	.825	.788 (.788–.797)
NV-AN-49-83	R3	.88	.864	.842	.813 (.813–.820)
NV-AL-47-83	R3	.90	.889	.875	.862 (.858–.866)
NV-AI-43-83	R3	.90	.889	.875	.862 (.858–.866)
13-108.5	R3	.92	.913	.905	.895 (.895–.900)
13-115.0	R3	.92	.913	.905	.895 (.895–.900)
NV-AG-42-83	R3	.93	.925	.919	.912 (.912–.925)
13-170.1	R3	.94	.936	.932	.927 (.927–.940)
13-140.0	R3	.95	.947	.945	.941 (.941–.950)
NV-AI-44-83	R3	.95	.947	.945	.941 (.941–.950)
13-119.7	R3	.97	.969	.968	.967 (.967–.970)
13-126.5	R3	.97	.969	.968	.967 (.967–.970)

https://doi.org/10.1346/CCMN.1986.0340203 Published online by Cambridge University Press

Table 4. Continued.

Sample[2]	Ordering	P_I	$P_{I,I}$	$P_{II,I}$	$P_{III,I}$
13-150.0	R3	.97	.969	.968	.967 (.967–.970)
13-146.0	R3	.98	.980	.979	.979 (.979–.980)
13-167.0	R3	.98	.980	.979	.979 (.979–.980)

[1] Fine size fraction (mostly <1 μm), oriented mount, glycolated. Parentheses = range of adequate fits.
[2] Bachelor Mountain Tuff, Creede, Colorado, described by Vergo (1984).

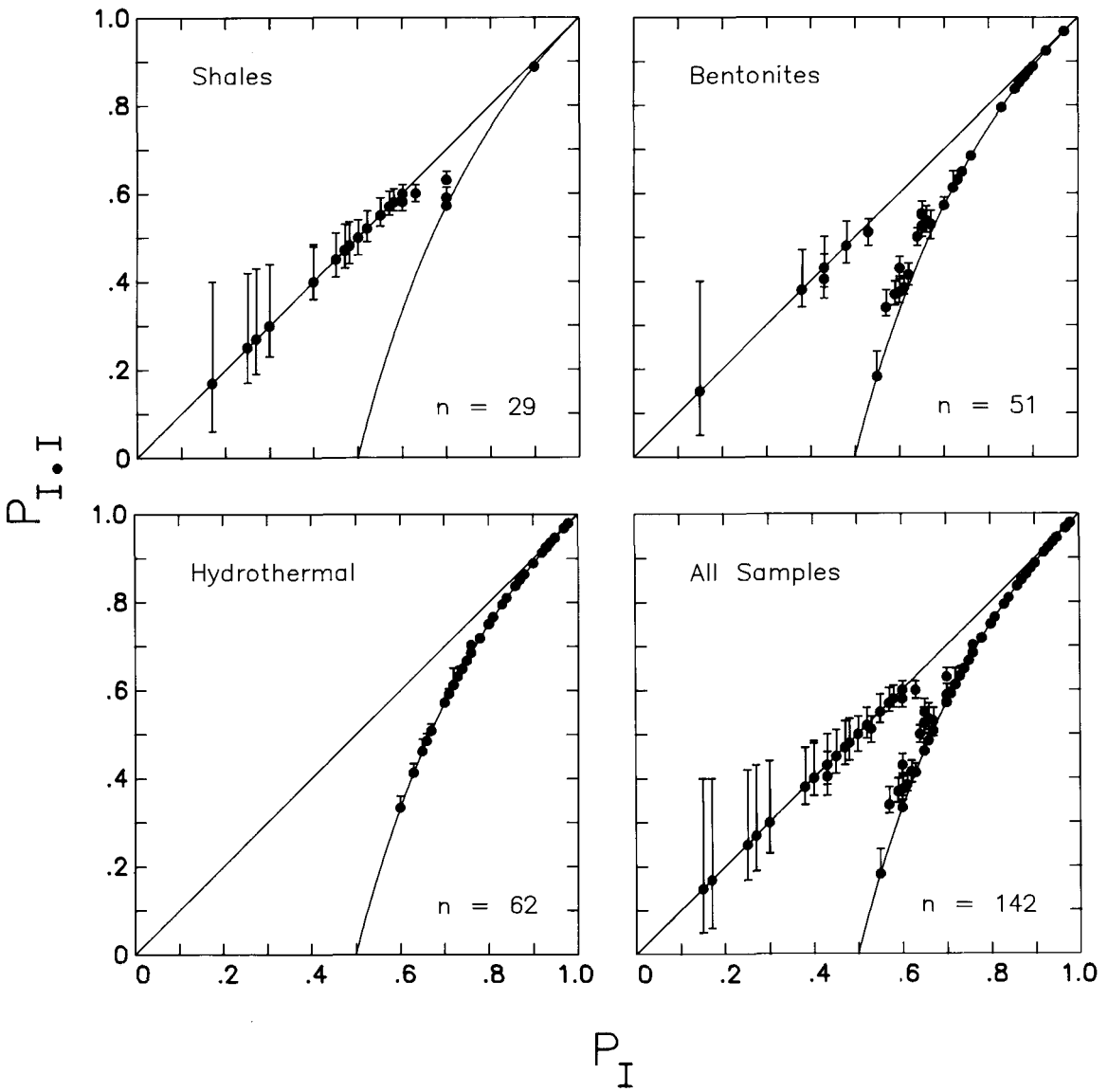

Figure 4. Mineralogical analyses of I/S from shales, bentonites, and hydrothermally altered tuffs, plotted on junction probability diagrams showing R1 layer arrangements. Points show best-fit values, as determined by X-ray powder diffraction modeling. Many points represent more than one sample. Bars show ranges of values which give reasonable diffraction models.

https://doi.org/10.1346/CCMN.1986.0340203 Published online by Cambridge University Press

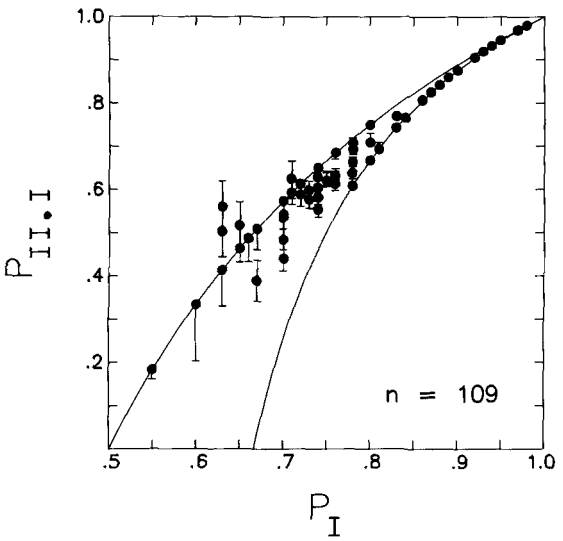

Figure 5. Analyses of R1-ordered I/S, plotted on R2 junction probability diagram.

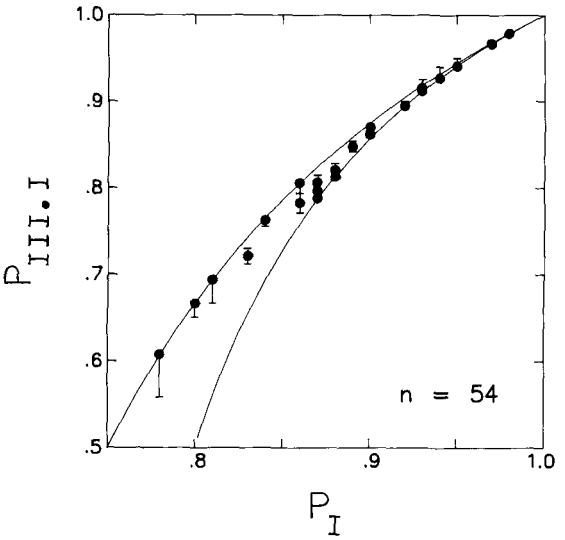

Figure 6. Analyses of R1- and R2-ordered I/S, plotted on R3 junction probability diagram.

at higher temperatures than those common under diagenetic conditions.

All samples, however, develop R2 and R3 ordering along similar pathways. Figure 5 shows that transition from R2-random to R2-ordered interlayering occurs gradually in R1-ordered I/S, from about 65–80% illite layers, but full R2 ordering appears only in I/S containing >75% illite layers. All samples containing ≧85% illite layers are fully R2 ordered. A few hydrothermal samples which show especially sharp low-angle peaks give better diffraction models assuming slight R2 segregation. This effect may be due to unusually thick crystallites, rather than true long-range segregation.

Development of R3 ordering (Figure 6) occurs in the range 85–90% illite layers, although some analyses of R2-ordered samples containing as little as 83% illite deviate slightly from the R3-random line. All samples containing >90% illite layers show moderate to strong R3 order.

ACKNOWLEDGMENTS

We appreciate many helpful discussions with D. G. Horton, R. C. Reynolds, and J. Hower. ARCO Oil and Gas Company, Exxon Production Research Company, and the University of Illinois Research Board sponsored this research. We thank the University of Illinois for use of its computer facilities, and Homestake Mining Company for access to mine and core samples. Terri Monnett typed the manuscript. The manuscript benefited from thoughtful reviews by D. D. Eberl, R. C. Reynolds, J. Środoń, and R. K. Stoessell.

REFERENCES

Altaner, S. P. (1985) Potassium metasomatism and diffusion in Cretaceous K-bentonites from the disturbed belt, northwestern Montana and in the Middle Devonian Tioga K-bentonite, eastern U.S.A.: Ph.D. dissertation, Univ. of Illinois, Urbana, Illinois, 193 pp.

Altaner, S. P., Whitney, G., Aronson, J. L., and Hower, J. (1984) A model for K-bentonite formation, evidence from zoned K-bentonites in the disturbed belt, Montana: *Geology* **12,** 412–415.

Boles, J. R. and Franks, S. G. (1979) Clay diagenesis in Wilcox sandstones of southwest Texas, implications of smectite diagenesis on sandstone cementation: *J. Sed. Petrol.* **49,** 55–70.

Bradley, W. F. (1950) The alternating layer sequence of rectorite: *Amer. Mineral.* **35,** 590–595.

Brindley, G. W. (1956) Allevardite, a swelling double-layer mica mineral: *Amer. Mineral.* **41,** 91–103.

Brun, J. and Chagnon, A. (1979) Rock stratigraphy and clay mineralogy of volcanic ash beds from the Black River and Trenton Groups (Middle Ordovician) of southern Quebec: *Canad. J. Earth Sci.* **16,** 1499–1507.

Hoffman, J. (1976) Regional metamorphism and K-Ar dating of clay minerals in Cretaceous sediments of the disturbed belt of Montana: Ph.D. dissertation, Case Western Reserve Univ., Cleveland, Ohio, 266 pp.

Horton, D. G. (1983) Argillic alteration associated with the Amethyst vein system, Creede Mining District: Ph.D. dissertation, Univ. of Illinois, Urbana, Illinois, 337 pp.

Hower, J., Eslinger, E. V., Hower, M., and Perry, E. A. (1976) Mechanism of burial metamorphism of argillaceous sediments, 1. Mineralogical and chemical evidence: *Geol. Soc. Amer. Bull.* **87,** 725–737.

Hower, J. and Mowatt, T. C. (1966) The mineralogy of illites and mixed-layer illite/montmorillonites: *Amer. Mineral.* **51,** 825–854.

Huff, W. D. and Türkmenöglü, A. G. (1981) Chemical characteristics and origin of Ordovician K-bentonites along the Cincinnati arch: *Clays & Clay Minerals* **29,** 113–123.

MacEwan, D. M. C. (1956) Fourier transform methods for studying scattering from lamellar systems, I. A direct method for analyzing interstratified mixtures: *Kolloid-Zeitschrift* **149,** 96–108.

MacEwan, D. M. C. (1958) Fourier transform methods for studying X-ray scattering from lamellar systems, II. The

calculation of X-ray diffraction effects for various types of interstratification: *Kolloid-Zeitschrift* **156,** 61–67.

Nadeau, P. H. and Reynolds, R. C. (1981) Burial and contact metamorphism in the Mancos shale: *Clays & Clay Minerals* **29,** 249–259.

Perry, E. A. (1969) Burial diagenesis in Gulf Coast pelitic sediments: Ph.D. dissertation, Case Western Reserve Univ., Cleveland, Ohio, 121 pp.

Perry, E. and Hower, J. (1970) Burial diagenesis in Gulf Coast pelitic sediments: *Clays & Clay Minerals* **18,** 165–177.

Pevear, D. R., Williams, V. E., and Mustoe, G. E. (1980) Kaolinite, smectite, and K-rectorite in bentonites, relation to coal rank at Tulameen, British Columbia: *Clays & Clay Minerals* **28,** 241–254.

Rettke, R. C. (1976) Clay mineralogy and clay mineral distribution patterns in Dakota Group sediments, northern Denver Basin, eastern Colorado and western Nebraska: Ph.D. dissertation, Case Western Reserve Univ., Cleveland, Ohio, 135 pp.

Reynolds, R. C. (1980) Interstratified clay minerals: in *Crystal Structures of Clay Minerals and their X-ray Identification,* G. W. Brindley and G. Brown, eds., Mineralogical Society, London, 249–303.

Reynolds, R. C. and Hower, J. (1970) The nature of interlayering in mixed-layer illite-montmorillonites: *Clays & Clay Minerals* **18,** 25–36.

Roberson, H. E. and Lahann, R. W. (1981) Smectite to illite conversion rates, effects of solution chemistry: *Clays & Clay Minerals* **29,** 129–135.

Środoń, J. (1984) X-ray powder diffraction identification of illitic materials: *Clays & Clay Minerals* **32,** 337–349.

Vergo, N. (1984) Wallrock alteration at the Bulldog Mountain Mine, Creede Mining District, Colorado: M.S. thesis, Univ. Illinois, Urbana, Illinois, 88 pp.

Weaver, C. E. (1956) The distribution and identification of mixed-layer clays in sedimentary rocks: *Amer. Mineral.* **41,** 202–221.

Weaver, C. E. (1959) The clay petrology of sediments: in *Clays and Clay Minerals, Proc. 6th Natl. Conf., Berkeley, California, 1957,* Ada Swineford, ed., Pergamon Press, New York, 154–187.

Weaver, C. E. and Beck, K. C. (1971) Clay water diagenesis during burial, how mud becomes gneiss: *Geol. Soc. Amer. Special Paper* **134,** 96 pp.

(Received 12 February 1985; accepted 3 July 1985; Ms. 1461)